

Chapter 11

Wind Driven Ocean Circulation

What drives the ocean currents? At first, we might answer, the winds drive the circulation. But if we think more carefully about the question, we might not be so sure. We might notice, for example, that strong currents, such as the North Equatorial Countercurrents in the Atlantic and Pacific Oceans go upwind. Spanish navigators in the 16th century noticed strong northward currents along the Florida coast that seemed to be unrelated to the wind. How can this happen? And, why are strong currents found offshore of east coasts but not offshore of west coasts?

Answers to the questions can be found in a series of three remarkable papers published from 1947 to 1951. In the first, Harald Sverdrup (1947) showed that the circulation in the upper kilometer or so of the ocean is directly related to the curl of the wind stress. Henry Stommel (1948) showed that the circulation in oceanic gyres is asymmetrical because the Coriolis force varies with latitude. Finally, Walter Munk (1950) added eddy viscosity and calculated the circulation of the upper layers of the Pacific. Together the three oceanographers laid the foundations for a modern theory of ocean circulation.

11.1 Sverdrup's Theory of the Oceanic Circulation

While Sverdrup was analyzing observations of equatorial currents, he came upon (11.7) below relating the curl of the wind stress to mass transport within the upper ocean. In deriving the relationship, Sverdrup assumed that the flow is stationary, and that the non-linear terms and lateral friction in the momentum equation are small. He assumed also that the flow is baroclinic and that the wind-driven circulation vanishes at some depth of no motion. From (8.9 and 8.14 a,b) the horizontal components of the momentum equation are:

$$\frac{\partial p}{\partial x} = f \rho v + \frac{\partial}{\partial z} \left(A_z \frac{\partial u}{\partial z} \right) \quad (11.1a)$$

$$\frac{\partial p}{\partial y} = -f \rho u + \frac{\partial}{\partial z} \left(A_z \frac{\partial v}{\partial z} \right) \quad (11.1b)$$

Sverdrup integrated these equations from the surface to a depth $-D$ equal to or greater than the depth at which the horizontal pressure gradient becomes zero. He defined:

$$\frac{\partial P}{\partial x} = \int_{-D}^0 \frac{\partial p}{\partial x} dz, \quad \frac{\partial P}{\partial y} = \int_{-D}^0 \frac{\partial p}{\partial y} dz, \quad (11.2a)$$

$$M_x \equiv \int_{-D}^0 \rho u(z) dz, \quad M_y \equiv \int_{-D}^0 \rho v(z) dz, \quad (11.2b)$$

where M_x, M_y are the mass transports in the wind-driven layer extending down to an assumed depth of no motion.

The horizontal boundary condition at the sea surface is the wind stress, and the boundary at depth $-D$ is zero stress because the currents go to zero:

$$\begin{aligned} \left(A_z \frac{\partial u}{\partial z} \right)_0 &= T_x & \left(A_z \frac{\partial u}{\partial z} \right)_{-D} &= 0 \\ \left(A_z \frac{\partial v}{\partial z} \right)_0 &= T_y & \left(A_z \frac{\partial v}{\partial z} \right)_{-D} &= 0 \end{aligned} \quad (11.3)$$

where T_x and T_y are the components of the wind stress.

Using these definitions and boundary conditions, (11.1) become:

$$\frac{\partial P}{\partial x} = f M_y + T_x \quad (11.4a)$$

$$\frac{\partial P}{\partial y} = -f M_x + T_y \quad (11.4b)$$

In a similar way, Sverdrup integrated the continuity equation (7.10) over the same vertical depth, assuming the vertical velocity at the surface and at depth $-D$ are zero, to obtain:

$$\frac{\partial M_x}{\partial x} + \frac{\partial M_y}{\partial y} = 0 \quad (11.5)$$

Differentiating (11.4a) with respect to y and (11.4b) with respect to x , subtracting, and using (11.5) gives:

$$\begin{aligned} \beta M_y &= \frac{\partial T_y}{\partial x} - \frac{\partial T_x}{\partial y} \\ \beta M_y &= \text{curl}_z(T) \end{aligned} \quad (11.6)$$

where $\beta \equiv \partial f / \partial y$ is the rate of change of Coriolis parameter with latitude, and where $\text{curl}_z(T)$ is the vertical component of the curl of the wind stress.

This is an important and fundamental result—the northward mass transport of wind driven currents is equal to the curl of the wind stress. Note that Sverdrup allowed f to vary with latitude. We will see later that this is essential.

If f varies only with latitude, then:

$$\begin{aligned} \frac{\partial f}{\partial x} &= 0 \\ \beta &\equiv \frac{\partial f}{\partial y} = \frac{2 \Omega \cos \varphi}{R} \end{aligned} \quad (11.7)$$

$$\frac{\partial^2 f}{\partial y^2} = -\frac{f}{R^2} \quad (11.8)$$

where R is Earth's radius and φ is latitude.

Over much of the open ocean, especially in the tropics, the wind is zonal and $\partial T_y / \partial x$ is sufficiently small that

$$M_y \approx -\frac{1}{\beta} \frac{\partial T_x}{\partial y} \quad (11.9)$$

Substituting (11.9) into (11.5), Sverdrup obtained:

$$\frac{\partial M_x}{\partial x} = -\frac{1}{2 \Omega \cos \varphi} \left(\frac{\partial T_x}{\partial y} \tan \varphi + \frac{\partial^2 T_x}{\partial y^2} R \right) \quad (11.10)$$

Sverdrup integrated this equation from a north-south eastern boundary at $x = 0$, assuming no flow into the boundary. This requires $M_x = 0$ at $x = 0$. Then

$$M_x = -\frac{\Delta x}{2 \Omega \cos \varphi} \left[\left\langle \frac{\partial T_x}{\partial y} \right\rangle \tan \varphi + \left\langle \frac{\partial^2 T_x}{\partial y^2} \right\rangle R \right] \quad (11.11)$$

where Δx is the distance from the eastern boundary of the ocean basin, and brackets indicate zonal averages of the wind stress.

To test his theory, Sverdrup compared transports calculated from known winds in the eastern tropical Pacific with transports calculated from hydrographic data collected by the *Carnegie* and *Bushnell* in October and November 1928, 1929, and 1939 between 22°N and 10°S along 80°W, 87°W, 108°W, and 109°W. The hydrographic data were used to compute P by integrating from a depth of $D = -1000$ m. The comparison, Figures 11.1 and 11.2, showed not only that the transports can be accurately calculated from the wind, but also that the theory predicts wind-driven currents going upwind.

Comments on Sverdrup's Solutions

1. Sverdrup assumed i) The internal flow in the ocean is geostrophic; ii) there is a uniform depth of no motion; and iii) Ekman's transport is correct. We have examined Ekman's theory in Chapter 9, and the geostrophic balance in Chapter 10. We know little about the depth of no motion in the tropical Pacific.

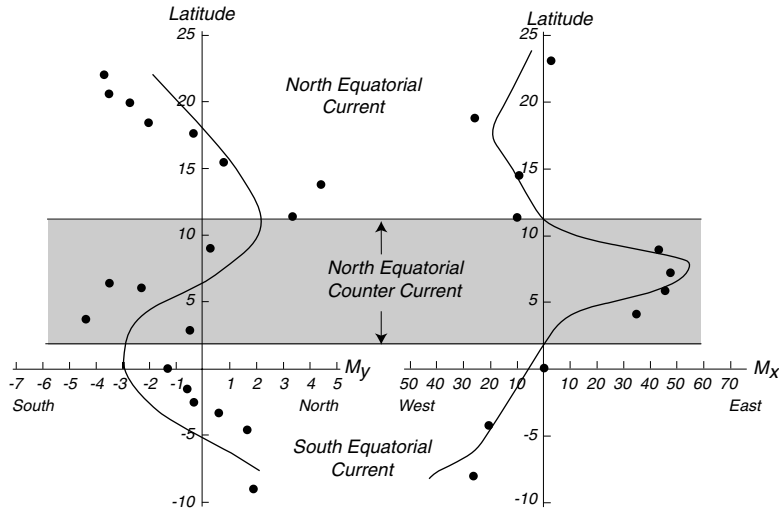


Figure 11.1 Mass transport in the eastern Pacific calculated from Sverdrup's theory using observed winds with 11.9 and 11.11 (solid lines) and pressure calculated from hydrographic data from ships with 11.4 (dots). Transport is in tons per second through a section one meter wide extending from the sea surface to a depth of one kilometer. Note the difference in scale between M_y and M_x (From Reid, 1948).

2. The solutions tend to be limited to the east side of the oceans because M_x grows with x . The result stems from neglecting friction which would eventually balance the wind-driven flow. Nevertheless, Sverdrup solutions have been used for describing the global system of surface currents. The

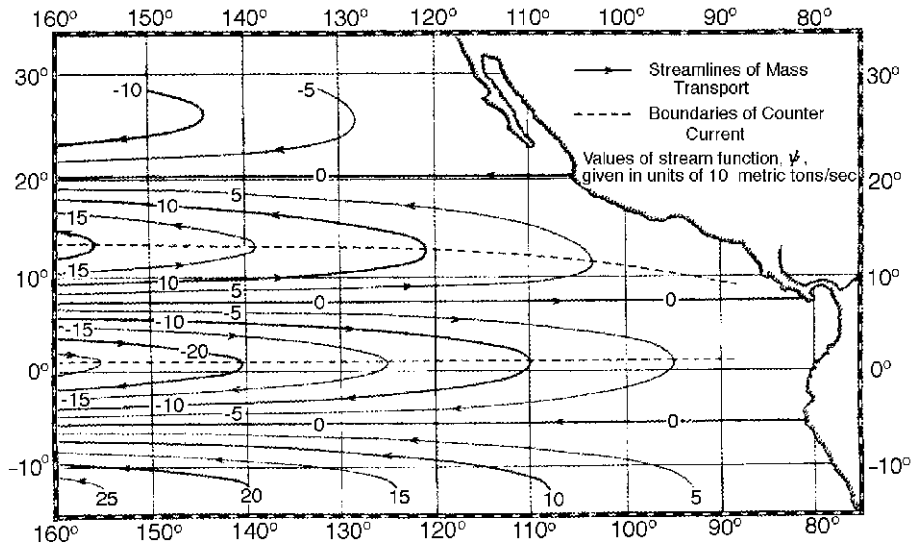


Figure 11.2 Streamlines of mass transport in the eastern Pacific calculated from Sverdrup's theory using mean annual wind stress (From Reid 1948).

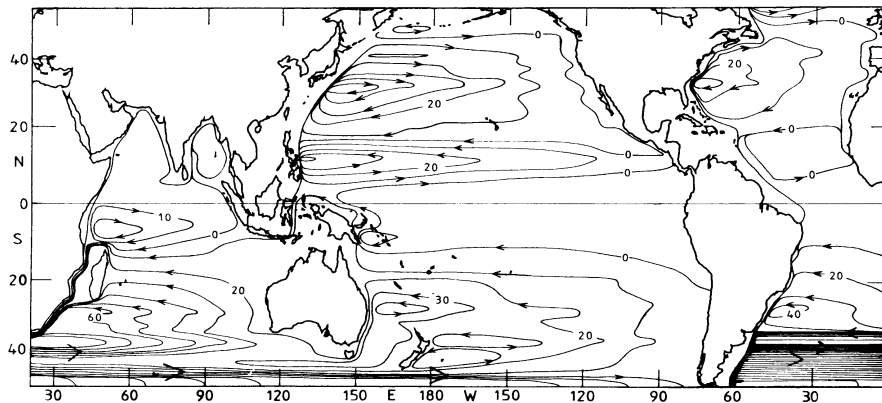


Figure 11.3 Depth-integrated Sverdrup transport applied globally using the wind stress from Hellerman and Rosenstein (1983). Contour interval is 10 Sverdrups. (From Tomczak and Godfrey, 1994)

solutions are applied throughout each basin all the way to the western limit of the basin. There, conservation of mass is forced by including north-south currents confined to a thin, horizontal boundary layer (Figure 11.3).

3. Only one boundary condition can be satisfied, no flow through the eastern boundary. More complete descriptions of the flow require more complete equations.
4. The solutions give no information on the vertical distribution of the current.
5. Results were based on data from one cruise plus climatological wind data assuming a steady state. Yet the flow varies in time and space, and the agreement of theory with observations could be due to chance.
6. Later calculations by Leetma, McCreary, and Moore (1981) using more recent wind data produces solutions with seasonal variability that agrees well with observations provided the level of no motion is at 500 m. If another depth were chosen, the results are not as good.
7. Wunsch (1996: §2.2.3) after carefully examining the evidence for a Sverdrup balance in the ocean concluded we do not have sufficient information to test the theory. He writes

The purpose of this extended discussion has not been to disapprove the validity of Sverdrup balance; rather, it was to emphasize the gap commonly existing in oceanography between a plausible and attractive theoretical idea and the ability to demonstrate its quantitative applicability to actual oceanic flow fields.—Wunsch (1996).

Wunsch, however, notes

Sverdrup's relationship is so central to theories of the ocean circulation that almost all discussions assume it to be valid without any

comment at all and proceed to calculate its consequences for higher-order dynamics ... it is difficult to overestimate the importance of Sverdrup balance—Wunsch (1996).

And the gap is shrinking. Measurements of mean stress in the equatorial Pacific (Yu and McPhaden, 1999) show that the flow there is in Sverdrup balance.

Stream Lines, Path Lines, and the Stream Function Before discussing further progress in understanding the ocean's wind-driven circulation, we need to introduce the concept of stream lines and the stream function (see Kundu, 1990: 51 & 66).

At each instant in time, we can represent the flow field in a fluid by a vector velocity at each point in space. The instantaneous curves that are everywhere tangent to the direction of the vectors are called the *stream lines* of the flow. If the flow is unsteady, the pattern of stream lines change with time.

The trajectory of a fluid particle, the path followed by a Lagrangean drifter, is called the *path line* in fluid mechanics. The path line is the same as the stream line for steady flow, and they are different for an unsteady flow.

We can simplify the description of two-dimensional, incompressible flows by use of the *stream function* ψ defined by:

$$u \equiv \frac{\partial \psi}{\partial y}, \quad v \equiv -\frac{\partial \psi}{\partial x}, \quad (11.12)$$

The stream function is often used because it is a scalar from which the vector velocity field can be calculated. This leads to simpler equations for some flows.

Stream functions are also useful for visualizing the flow. At each instant, the flow is parallel to lines of constant ψ . Thus if the flow is steady, the lines of constant stream function are the paths followed by water parcels.

The volume rate of flow between any two stream lines of a steady flow is $d\psi$, and the volume rate of flow between two stream lines ψ_1 and ψ_2 is equal to $\psi_1 - \psi_2$. To see this, consider an arbitrary line $dx = (dx, dy)$ between two stream lines (Figure 11.4). The volume rate of flow between the stream lines is:

$$v dx + (-u) dy = -\frac{\partial \psi}{\partial x} dx - \frac{\partial \psi}{\partial y} dy = -d\psi \quad (11.13)$$

and the volume rate of flow between the two stream lines is numerically equal to the difference in their values of ψ .

Now, lets apply the concepts to satellite-altimeter maps of the oceanic topography. Referring back to the discussion of surface geostrophic currents observed by satellite altimeters, we wrote (10.10)

$$\begin{aligned} u_s &= -\frac{g}{f} \frac{\partial \zeta}{\partial y} \\ v_s &= \frac{g}{f} \frac{\partial \zeta}{\partial x} \end{aligned} \quad (11.14)$$

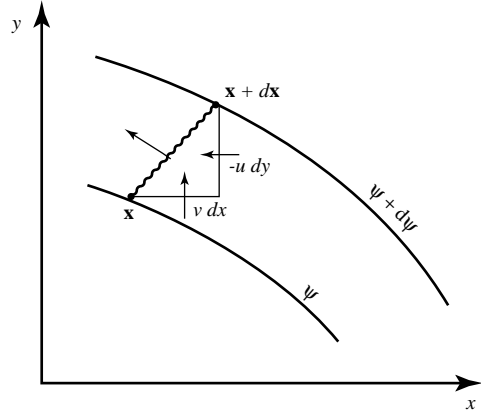


Figure 11.4 Volume transport between stream lines in a two-dimensional, steady flow (From Kundu, 1990).

Comparing (11.14) with (11.12) it is clear that

$$\psi = -\frac{g}{f} \zeta \tag{11.15}$$

and the sea surface is a stream function scaled by g/f . Turning to Figure 10.6, the lines of constant height are stream lines, and flow is along the lines. The surface geostrophic transport is proportional to the difference in height, independent of distance between the stream lines. The same statements apply to Figure 10.9, except that the transport is relative to transport at the 1000 decibars surface, which is roughly one kilometer deep.

In addition to the stream function, oceanographers use the mass-transport stream function Ψ defined by:

$$M_x \equiv \frac{\partial \Psi}{\partial y}, \quad M_y \equiv -\frac{\partial \Psi}{\partial x} \tag{11.16}$$

This is the function shown in Figures 11.2 and 11.3.

11.2 Stommel's Theory of Western Boundary Currents

At the same time Sverdrup was beginning to understand circulation in the eastern Pacific, Stommel was beginning to understand why western boundary currents occur in ocean basins. To study the circulation in the North Atlantic, Stommel (1948) used essentially the same equations used by Sverdrup (11.1, 11.2, and 11.3) but he added a simple bottom stress proportional to velocity to (11.3):

$$\left(A_z \frac{\partial u}{\partial z} \right)_0 = -T_x = -F \cos(x b/y) \quad \left(A_z \frac{\partial u}{\partial z} \right)_D = -R u \tag{11.17a}$$

$$\left(A_z \frac{\partial v}{\partial z} \right)_0 = -T_y = 0 \quad \left(A_z \frac{\partial v}{\partial z} \right)_D = -R v \tag{11.17b}$$

where F and R are constants.

Stommel calculated steady-state solutions for flow in a rectangular basin $0 \leq y \leq b$, $0 \leq x \leq \lambda$ of constant depth D filled with water of constant density. His first solution was for a non-rotating Earth. This solution had a symmetric flow pattern with no western boundary current (Figure 11.5, left). Next, Stommel assumed a constant rotation, which again led to a symmetric solution with no western boundary current. Finally, he assumed that the Coriolis force varies with latitude. This led to a solution with western intensification (Figure 11.5, right). Stommel suggested that the crowding of stream lines in the west indicated that the variation of Coriolis force with latitude may explain why the Gulf Stream is found in the ocean. We now know that the variation of Coriolis force with latitude is required for the existence of the western boundary current, and that other models for the flow which use different formulations for friction, lead to western boundary currents with different structure. Pedlosky (1987, Chapter 5) gives a very useful, succinct, and mathematically clear description of the various theories for western boundary currents. Müller (1995) gives a more mathematical description.

In the next chapter, we will see that Stommel's results can also be explained in terms of vorticity—wind produces clockwise torque (vorticity), which must be balanced by a counterclockwise torque produced at the western boundary.

11.3 Munk's Solution

Sverdrup's and Stommel's work suggested the dominant processes producing a basin-wide, wind-driven circulation. Munk (1950) built upon this foundation, adding information from Rossby (1936) on lateral eddy viscosity, to obtain a solution for the circulation within an ocean basin. Munk used Sverdrup's idea of a vertically integrated mass transport flowing over a motionless deeper layer. This simplified the mathematical problem, and it is more realistic. The ocean currents are concentrated in the upper kilometer of the ocean, they are not barotropic and independent of depth. To include friction, Munk used lateral

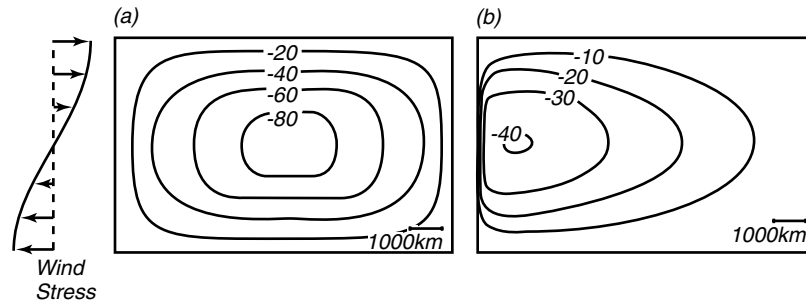


Figure 11.5 Stream function for flow in a basin as calculated by Stommel (1948). **Left:** Flow for non-rotating basin or flow for a basin with constant rotation. **Right:** Flow when rotation varies linearly with y .

eddy friction with constant $A_H = A_x = A_y$. Equations (11.1) become:

$$\frac{\partial p}{\partial x} = f \rho v + \frac{\partial}{\partial z} \left(A_z \frac{\partial u}{\partial z} \right) + A_H \frac{\partial^2 u}{\partial x^2} \quad (11.18a)$$

$$\frac{\partial p}{\partial y} = -f \rho u + \frac{\partial}{\partial z} \left(A_z \frac{\partial v}{\partial z} \right) + A_H \frac{\partial^2 v}{\partial y^2} \quad (11.18b)$$

Munk integrated the equation from a depth $-D$ to the surface at $z = z_0$ which is similar to Sverdrup's integration except that the surface is not at $z = 0$. Munk assumed that currents at the depth $-D$ vanish, and that (11.3) apply at the horizontal boundaries at the top and bottom of the layer.

To simplify the equations, Munk used the mass-transport stream function (11.16), and he proceeded along the lines of Sverdrup. He eliminated the pressure term by taking the y derivative of (11.18a) and the x derivative of (11.18b) to obtain the equation for mass transport:

$$\underbrace{A_H \nabla^4 \Psi}_{\text{Friction}} - \underbrace{\beta \frac{\partial \Psi}{\partial x}}_{\text{Sverdrup Balance}} = -\text{curl}_z \quad (11.19)$$

where

$$\nabla^4 = \frac{\partial^4}{\partial x^4} + 2 \frac{\partial^4}{\partial x^2 \partial y^2} + \frac{\partial^4}{\partial y^4} \quad (11.20)$$

is the biharmonic operator. Equation (11.19) is the same as (11.6) with the addition of the lateral friction term A_H . The friction term is large close to a lateral boundary where the horizontal derivatives of the velocity field are large, and it is small in the interior of the ocean basin. Thus in the interior, the balance of forces is the same as that in Sverdrup's solution.

Equation (11.19) is a fourth-order partial differential equation, and four boundary conditions are needed. Munk assumed the flow at a boundary is parallel to a boundary and that there is no slip at the boundary:

$$\Psi_{bdry} = 0, \quad \left(\frac{\partial \Psi}{\partial n} \right)_{bdry} = 0 \quad (11.21)$$

where n is normal to the boundary. Munk then solved (11.19) with (11.21) assuming the flow was in a rectangular basin extending from $x = 0$ to $x = r$, and from $y = -s$ to $y = +s$. He further assumed that the wind stress was zonal and in the form:

$$\begin{aligned} T &= a \cos ny + b \sin ny + c \\ n &= j \pi/s, \quad j = 1, 2, \dots \end{aligned} \quad (11.22)$$

Munk's solution (Figure 11.6) shows the dominant features of the gyre-scale circulation in an ocean basin. It has a circulation similar to Sverdrup's in the

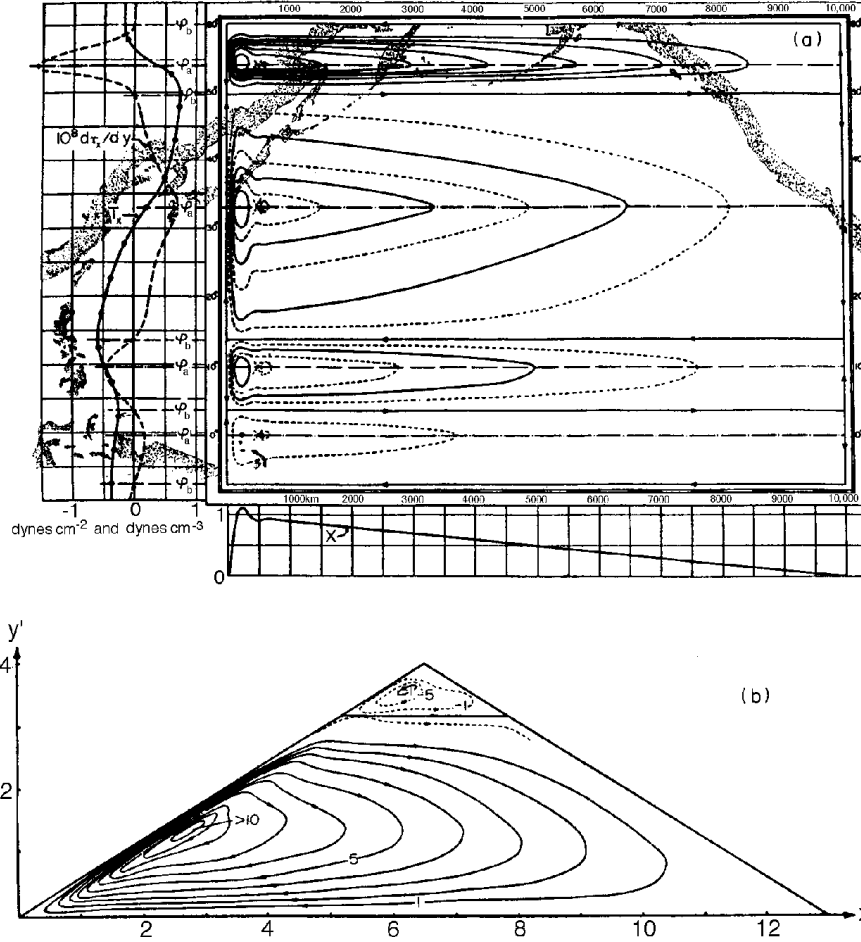


Figure 11.6 **Upper Left:** Mean annual wind stress $T_x(y)$ over the Pacific and the curl of the wind stress. **Upper Right:** The mass transport stream function for a rectangular basin calculated by Munk (1950) using observed wind stress for the Pacific. Contour interval is $10 \times 10^6 \text{ m}^3/\text{s} = 10$ Sverdrups. The total transport between the coast and any point x, y is $\psi(x, y)$. The transport in the relatively narrow northern section is greatly exaggerated. **Lower Right:** North-South component of the mass transport. **Bottom:** The solution for a triangular basin. (From Munk, 1950).

eastern parts of the ocean basin and a strong western boundary current in the west. Using $A_H = 5 \times 10^3 \text{ m}^2/\text{s}$ gives a boundary current roughly 225 km wide with a shape similar to the flow observed in the Gulf Stream and the Kuroshio (Figure 11.7).

The transport in western boundary currents is independent of A_H , and it depends only on (11.6) integrated across the width of the ocean basin. Hence, it depends on the width of the ocean, the curl of the wind stress, and β . Using the best available estimates of the wind stress, Munk calculated that the Gulf Stream should have a transport of 36 Sv and that the Kuroshio should have a

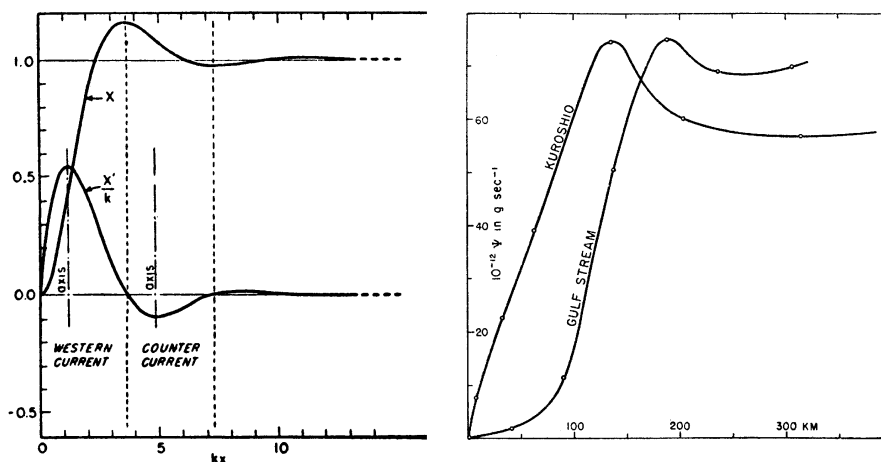


Figure 11.7 **Left:** Northward mass transport X and transport per unit length X'/k in the ocean calculated by Munk (1950). **Right:** Mass transport stream function y computed from hydrographic data across the Kuroshio and Gulf Stream. The Gulf Stream data were collected by the Atlantis at stations 1225–1231 in April 1931; the Kuroshio data were collected by the Mansyu at stations 429–434 in January 1927. $x = 0$ is at the continental shelf. (From Munk, 1950).

transport of 39 Sv. The values are about one half of the measured values of the flow available to Munk. This is very good agreement considering the wind stress was not well known.

Recent recalculations show good agreement except for the region offshore of Cape Hattaras where there is a strong recirculation. Munk's solution was based on wind stress averaged over 5° squares. This underestimated the curl of the stress. Leetma and Bunker (1978) used modern drag coefficient and $2^\circ \times 5^\circ$ averages of stress to obtain 32 Sv transport in the Gulf Stream, a value very close to that calculated by Munk.

11.4 Observed Circulation in the Atlantic

The theories by Sverdrup, Munk, and Stommel describe a very simple flow. But the ocean is much more complicated. To see just how complicated the flow is at the surface, let's look at a whole ocean basin, the North Atlantic. I have chosen this region because it is the best observed, and because mid-latitude processes in the Atlantic are similar to mid-latitude processes in the other oceans. Thus, for example, we use the Gulf Stream as an example of a western boundary current.

Let's begin with the Gulf Stream to see how our understanding of ocean currents has evolved. Of course, we can't look at all aspects of the flow. You can find out much more by reading Tomczak and Godfrey (1994) book on *Regional Oceanography: An Introduction*.

North Atlantic Circulation The North Atlantic is the most thoroughly studied ocean basin. There is an extensive body of theory to describe most aspects of the circulation, including flow at the surface, in the thermocline, and at depth,

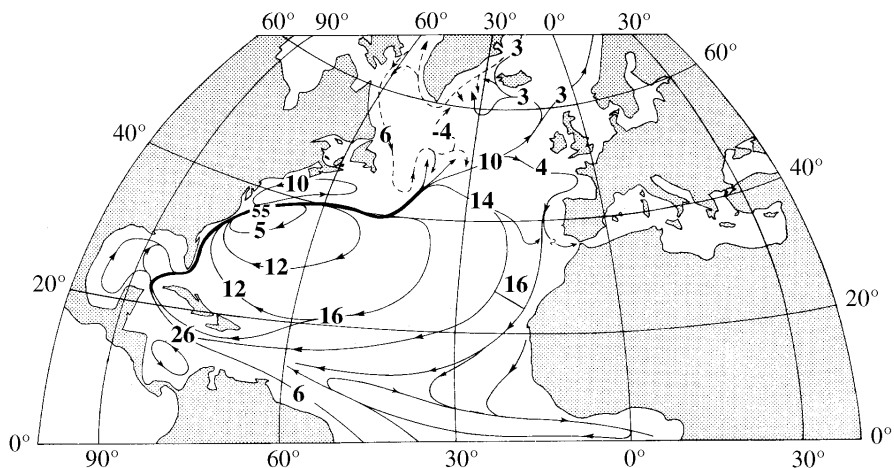


Figure 11.8 Schematic of currents in the North Atlantic showing major surface currents. Values are transport in units of $10^6 \text{ m}^3/\text{s}$ (From Sverdrup, Johnson, and Fleming 1942: Fig. 187).

together with an extensive body of field observations. By looking at figures depicting the circulation, we can learn more about the circulation, and by looking at the figures produced over the past few decades we can trace an ever more complete understanding of the circulation.

Let's begin with the traditional view of the time-averaged flow in the North Atlantic based mostly on hydrographic observations of the density field (Figure 2.7). It is a contemporary view of the mean circulation of the entire ocean based on a century of more of observations. Because the figure includes all the oceans, perhaps it is overly simplified. So, let's look then at a similar view of the mean circulation of just the North Atlantic (Figure 11.8).

The figure shows a broad, basin-wide, mid latitude gyre as we expect from Sverdrup's theory described in §11.1. In the west, a western boundary current, the Gulf Stream, completes the gyre. In the north a subpolar gyre includes the Labrador current. An equatorial current system and countercurrent are found at low latitudes with flow similar to that in the Pacific. Note, however, the strong cross equatorial flow in the west which flows along the northeast coast of Brazil toward the Caribbean.

If we look closer at the flow in the far north Atlantic (Figure 11.9) we see that the flow is still more complex. This figure includes much more detail of a region important for fisheries and commerce. Because it is based on an extensive base of hydrographic observations, is this reality? For example, if we were to drop a Lagrangean float into the Atlantic would it follow the streamline shown in the figure?

To answer the question, let's look at the tracks of a 110 buoys drifting on the sea surface compiled by Phil Richardson (Figure 11.10 top). The tracks give a very different view of the currents in the North Atlantic. It is hard to distinguish the flow from the jumble of lines, sometimes called spaghetti tracks. Clearly, the flow is very turbulent, especially in the Gulf Stream, a fast, western-boundary

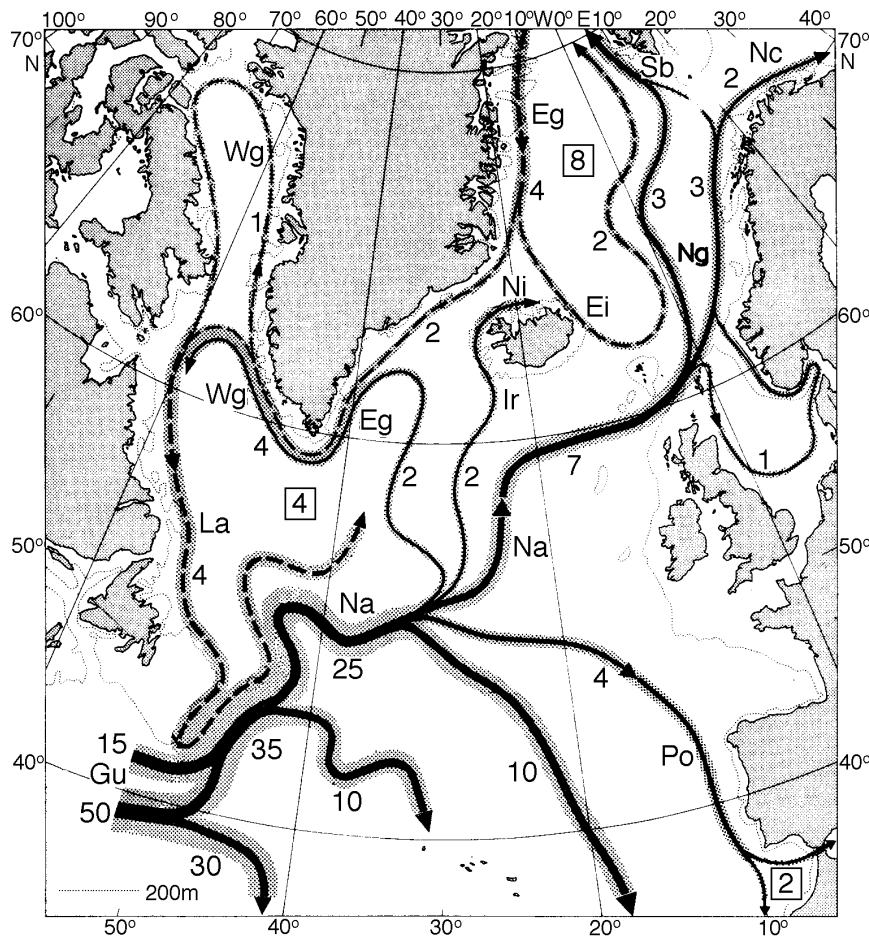


Figure 11.9 Detailed schematic of currents in the North Atlantic showing major surface currents. The numbers give the transport in units on $10^6 m^3/s$ from the surface to a depth of $10^6 m^3/s$. **Eg**: East Greenland Current; **Ei**: East Iceland Current; **Gu**: Gulf Stream; **Ir**: Irminger Current; **La**: Labrador Current; **Na**: North Atlantic Current; **Nc**: North Cape Current; **Ng**: Norwegian Current; **Ni**: North Iceland Current; **Po**: Portugal Current; **Sb**: Spitzbergen Current; **Wg**: West Greenland Current. Numbers within squares give sinking water in units on $10^6 m^3/s$. Solid Lines: Relatively warm currents. Broken Lines: Relatively cold currents. (From Dietrich, et al. 1980).

current. Furthermore, the turbulent eddies seem to have a diameter of a few degrees. This is much different than turbulence in the atmosphere. In the air, the large eddies are called storms, and storms have diameters of 10° – 20° . Thus oceanic “storms” are much smaller than atmospheric storms.

Perhaps we can see the mean flow if we average the drifter tracks. What happens when Richardson averages the tracks through $2^\circ \times 2^\circ$ boxes? The averages (Figure 11.10 bottom) begin to show some trends, but note that in some regions, such as east of the Gulf Stream, adjacent boxes have very different means, some having currents going in different directions. This indicates the

flow is so variable, that the average is not stable; and 40 or more observations do not yields a stable mean value. Overall, Richardson finds that the kinetic energy of the eddies is 8 to 37 times larger than the kinetic energy of the mean flow. Thus the oceanic turbulence is very different than laboratory turbulence. In the lab, the mean flow is typically much faster than the eddies.

Further work by Richardson (1993) based on subsurface buoys freely drifting at depths between 500 and 3,500 m, shows that the current extends deep below the surface, and that typical eddy diameter is 80 km.

Gulf Stream Recirculation Region If we look closely at figure 11.9 we see that the transport in the Gulf Stream increases from 26 Sv in the Florida Strait (between Florida and Cuba) to 55 Sv offshore of Cape Hattaras. Later measurements showed the transport increases from 30 Sv in the Florida Strait to 150 Sv near 40°N.

The observed increase, and the large transport off Hatteras, disagree with transports calculated from Sverdrup's theory. Theory predicts a much smaller maximum transport of 30 Sv, and that the maximum ought to be near 28°N. Now we have a problem: What causes the high transports near 40°N?

Niiler (1987) summarizes the theory and observations. First, there is no hydrographic evidence for a large influx of water from the Antilles Current that flows north of the Bahamas and into the Gulf Stream. This rules out the possibility that the Sverdrup flow is larger than the calculated value, and that the flow bypasses the Gulf of Mexico. The flow seems to come primarily from the Gulf Stream itself. The flow between 60°W and 55°W is to the south. The water then flows south and west, and rejoins the Stream between 65°W and 75°W. Thus, there are two subtropical gyres: a small gyre directly south of the Stream centered on 65°W, called the Gulf Stream recirculation region, and the broad, wind-driven gyre near the surface seen in figure 11.8 that extends all the way to Europe.

The Gulf Stream recirculation carries two to three times the mass of the broader gyre. Current meters deployed in the recirculation region show that the flow extends to the bottom. This explains why the recirculation is weak in the maps calculated from hydrographic data. Currents calculated from the density distribution give only the baroclinic component of the flow, and they miss the component that is independent of depth, the barotropic component.

The Gulf Stream recirculation is driven by the potential energy of the steeply sloping thermocline at the Gulf Stream. The depth of the 27.00 sigma-theta (σ_θ) surface drops from 250 meters near 41°N in figure 10.12 to 800 m near 38°N south of the Stream. Eddies in the Stream convert the potential energy to kinetic energy through baroclinic instability. The instability leads to an interesting phenomena: negative viscosity. The Gulf Stream accelerates not decelerates. It acts as though it were under the influence of a negative viscosity. The same process drives the jet stream in the atmosphere. The steeply sloping density surface separating the polar air mass from mid-latitude air masses at the atmosphere's polar front also leads to baroclinic instability. For more on this fascinating see Starr's (1968) book on *Physics of Negative Viscosity Phenomena*.

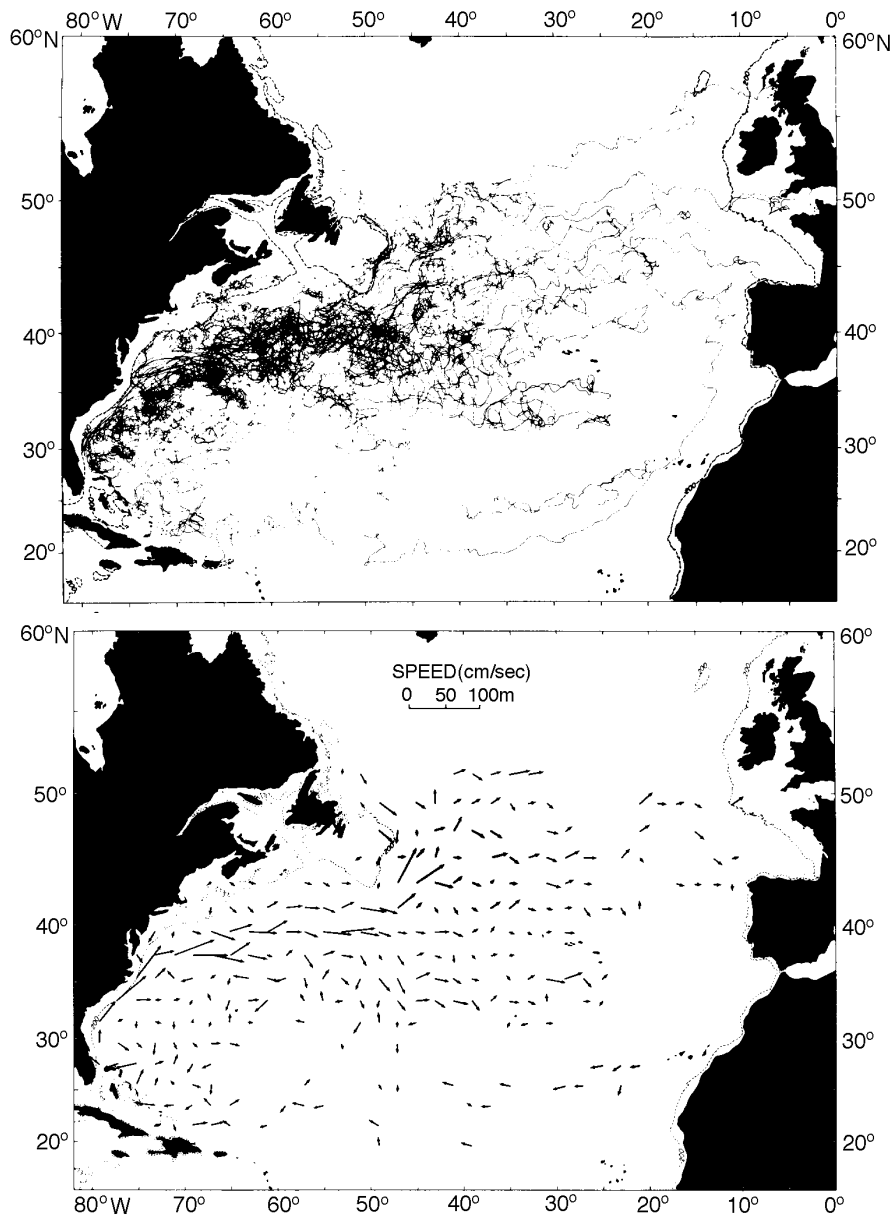


Figure 11.10 **Top** Tracks of 110 drifting buoys deployed in the western North Atlantic. **Bottom** Mean velocity of currents in $2^\circ \times 2^\circ$ boxes calculated from tracks above. Boxes with fewer than 40 observations were omitted. Length of arrow is proportional to speed. Maximum values are near 0.6 m/s in the Gulf Stream near $37^\circ\text{N } 71^\circ\text{W}$. (From Richardson 1983).

Let's look at this process in the Gulf Stream (figure 11.11). The strong current shear in the Stream causes the flow to begin to meander. The meander intensifies, and eventually the Stream throws off a ring. Those on the south

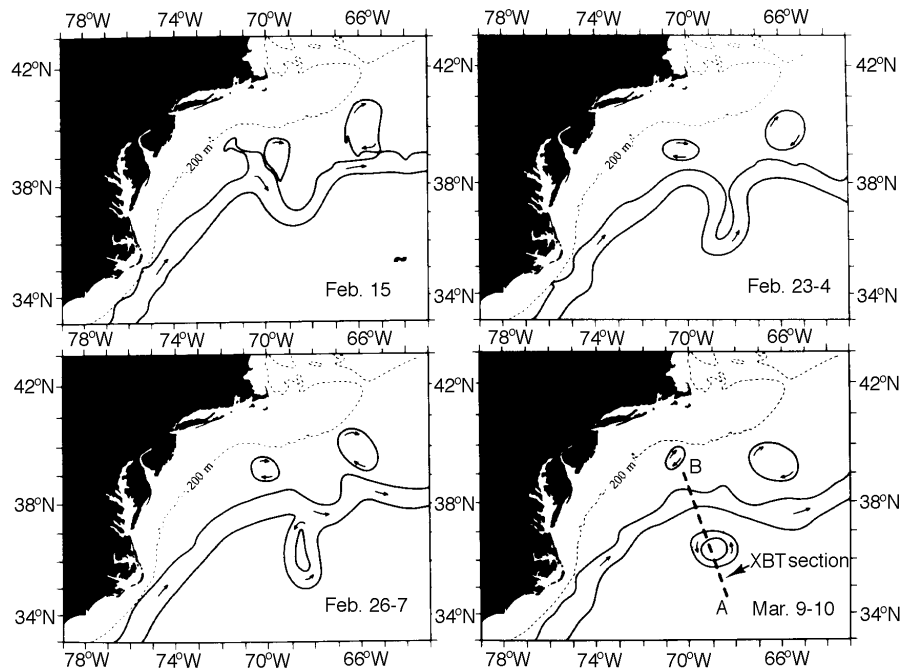


Figure 11.11 Gulf Stream meanders lead to the formation of a spinning eddy, a ring. Notice that rings have a diameter of about 1° (From Ring Group, 1981).

side drift southwest, and eventually merge with the stream several months later (figure 11.12). The process occurs all along the recirculation region, and satellite images show nearly a dozen or so rings occur north and south of the stream (figure 11.12). In the south Atlantic, there is another western boundary current, the Brazil Current that completes the Sverdrup circulation in that basin. Between the flow in the north and south Atlantic lies the equatorial circulation similar to the circulation in the Pacific. Before we can complete our description of the Atlantic, we need to look at the Antarctic Circumpolar Current.

11.5 Important Concepts

1. The theory for wind-driven, geostrophic currents was first outlined in a series of papers by Sverdrup, Stommel, and Munk between 1947 and 1951.
2. They showed that realistic currents can be calculated only if the Coriolis parameter varies with latitude.
3. Sverdrup showed that the curl of the wind stress is driven by a northward mass transport, and that this can be used to calculate currents in the ocean away from western boundary currents.
4. Stommel showed that western boundary currents are required for flow to circulate around an ocean basin when the Coriolis parameter varies with latitude.

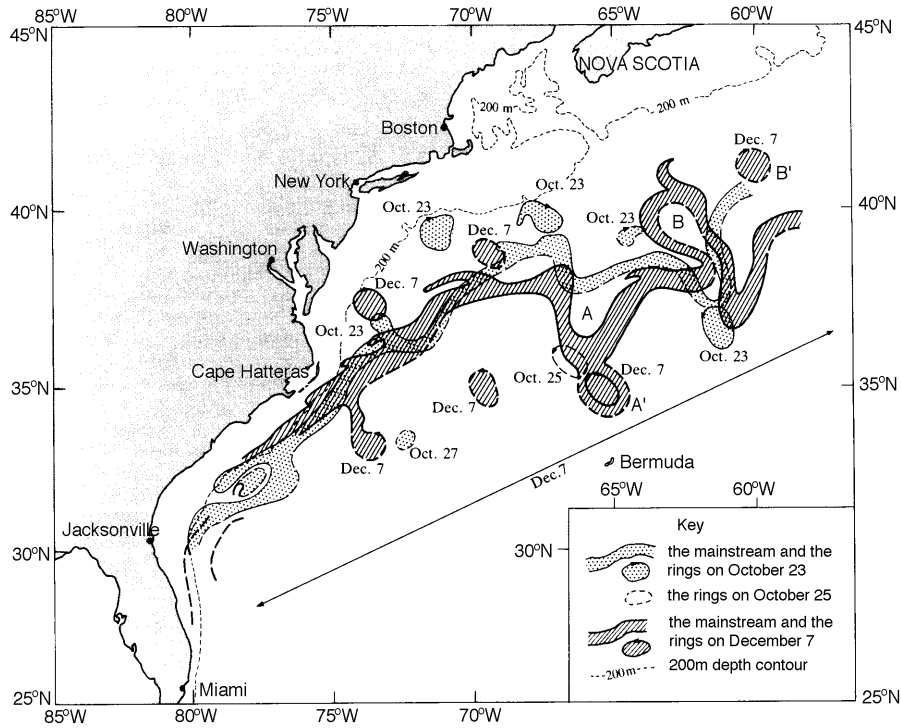


Figure 11.12 Sketch of the position of the Gulf Stream, warm core, and cold core eddies observed in infrared images of the sea surface collected by the infrared radiometer on NOAA-5 in October and December 1978 (from Tolmazin, 1985: 91).

5. Munk showed how to combine the two solutions to calculate the wind-driven geostrophic circulation in an ocean basin. In all cases, the current is driven by the curl of the wind stress.
6. The observed circulation in the ocean is very turbulent. many years of observations may need to be averaged together to obtain a stable map of the mean flow.
7. The Gulf Stream is a region of baroclinic instability in which turbulence accelerates the stream. This creates a Gulf Stream recirculation. Transports in the recirculation region are much larger than transports calculated from the Sverdrup-Munk theory.